

A grid of Non-LTE model atmospheres and synthetic spectra for DO white dwarfs

M.I. Nouh and D.A. Fouda

*National Research Institute of Astronomy and Geophysics, 11421 Helwan,
Cairo, Egypt (E-mail: nouh@nriag.sci.eg)*

Received: October 10, 2006; Accepted: June 26, 2007

Abstract. We present a grid of NLTE model atmospheres and synthetic spectra for hot helium-rich white dwarfs in order to elucidate the nature and characteristics of the progenitors of the DO white dwarfs. The grid coverage is $50000 \leq T_{eff} \leq 120000$ K with a step of 2500 K and $7 \leq \log g \leq 8.5$ with a step of 0.25 dex, for three helium abundance values (He/H): 10^2 , 10^3 and 10^4 by number. The spectra are synthesized with a sampling of 0.1 Å and covering the wavelength range from 3000 to 7000 Å. An application to the observed spectra is given.

Key words: stars: white dwarfs – model atmospheres – NLTE effect

1. Introduction

A majority of stars will eventually end their lives as white dwarfs. These faint stellar remnants can be used in many different investigations. Although white dwarfs are faint, studying them is becoming easier with larger telescopes and improved instrumentation.

White dwarfs can be divided into two basic distinct spectroscopic sequences, the DA and non-DA white dwarfs. DA white dwarfs display a pure hydrogen spectrum and can be found for all temperatures of the white dwarf cooling sequence, Koester (2002).

Non-DA white dwarfs comprises DO ($T_{eff} > 45000$ K), DB (11000 K $< T_{eff} < 30000$ K) and DC ($T_{eff} < 11000$ K) white dwarfs. DO white dwarfs display a pure He II lines spectrum at the hot end ($T_{eff} \geq 100000$ K) and He I/He II lines for the cool end. DB white dwarfs display a pure He I lines spectrum. DC white dwarfs could be found for $T_{eff} < 11000$ K and show featureless spectra (continuum spectra).

Model atmosphere analysis of hot helium-rich white dwarfs (DO) was performed by many authors. Wesemael (1981) computed pure helium models to investigate the nature and properties of helium-rich white dwarfs. Wesemael et al. (1985) analyzed DO white dwarfs with a help of a grid of LTE model atmospheres.

The effect of NLTE on the calculation of model atmosphere were analyzed by Dreizler and Werner (1996). Hügelmeyer et al. (2005) presented a grid of NLTE model atmosphere for a spectral analysis of DO white dwarfs from the Sloan Digital Sky Survey (SDSS).

Kubat (1997) studied the effect of increasing helium abundance on the temperature structure of NLTE model atmospheres of hot white dwarfs with the effective temperature $T_{eff} = 100000$ K and $\log g = 7.5$. He found quite dramatic changes in the temperature structure even for very low abundances of helium. Kubat (1995) also investigated the sphericity effects in the atmospheres of white dwarfs and found that they are not drastic but they are not absent.

In the present paper, a grid of NLTE model atmospheres and synthetic spectra for hot helium-rich white dwarfs are presented in order to elucidate the nature and characteristics of the progenitors of the DO white dwarfs. The grid coverage is $50000 \leq T_{eff} \leq 120000$ K with a step of 2500 K and $7 \leq \log g \leq 8.5$ with a step of 0.25 dex, for three helium abundance (by number relative to hydrogen) values (He/H): 10^2 , 10^3 and 10^4 . The spectra are synthesized with a sampling of 0.1 Å and covering the wavelength range from 3000 to 7000 Å.

The organization of the paper is as follows: Section 2 deals with the codes implemented for the present calculation of the model grid and synthetic spectra. In section 3 the physical parameters of the models and spectral behavior of the synthetic spectra are outlined. Section 4 is devoted to the application to the observed spectra.

2. Generating the model grid and synthetic spectra

The atmospheric structure is modelled using the TLUSTY code (version 200; Hubeny 1988; Hubeny and Lanz 1992, 1995, 2003; Lanz and Hubeny 2001; Lanz et al. 2003). TLUSTY considers the atmosphere as plane-parallel, horizontally homogeneous in both radiative and hydrostatic equilibrium. Departures from local thermodynamic equilibrium (LTE) are allowed for an arbitrary set atomic and ionic energy levels, Lanz and Hubeny (2006). The program solves the basic equations of radiative transfer, hydrostatic equilibrium, radiative equilibrium, statistical equilibrium, charge and particle conservation. The program treats convection with the mixing length theory.

We use to synthesis the spectra the code SYNSPEC (version 43, Hubeny and Lanz, 2003) which is a general spectrum synthesis program. The input model atmospheres to SYNSPEC could be taken from TLUSTY or from the literature. Then the program solves the radiative transfer equation wavelength by wavelength in a specified wavelength range and with a specified wavelength resolution.

In the present calculations, we consider that the atmosphere consists only from hydrogen and helium, the heavier elements have been neglected.

Hydrogen is represented essentially exactly: the first eight principal quantum numbers are treated separately, while the upper levels are merged into a single non-LTE level accounting for a level dissolution as described by Hubeny, Hummer and Lanz (1994). All lines between the first 8 bound levels are included, assuming an approximate Stark profile for the Lyman and Balmer series (Hubeny et al. 1994) and a Doppler profile for the other lines.

Neutral helium is represented by a 14-level model atom, which incorporates all singlet and triplet levels up to $n = 8$. The five lowest levels are included individually; singlet and triplet levels are grouped separately from $n = 3$ to $n = 5$, $n = 6$, $n = 7$, and 8 have formed three superlevels. The first 14 levels of He II are explicitly treated. Also, approximate Stark profiles are assumed.

For the purpose of the present investigation, we constructed the following sequence of the models: LTE-gray (LTE gray model atmosphere), LTE, NLTE-C (NLTE model atmosphere for continua) and NLTE-L (NLTE model atmosphere for lines).

The grid consists of 609 models, the effective temperature (T_{eff}) spans the range from 50000 K to 120000 K with a step of 2500 K. The surface gravity ($\log g$) spans the range from 7 to 8.5 with a step of 0.25 dex. The grid has been calculated for the helium abundance (by number relative to hydrogen) He/H: 10^2 , 10^3 and 10^4 . The spectra are synthesized with a sampling of 0.1 Å and covering the wavelength range from 3000 Å to 7000 Å.

3. Spectral properties of the grid

3.1. Properties of models

The effect of the NLTE on the temperature stratification is displayed in Figure 1 for cool model at $T_{eff} = 50000$ K, $\log g = 8$ and He/H = 10^2 , and in Figure 2 for hot model at $T_{eff} = 100000$ K, $\log g = 8$ and He/H = 10^2 , the effect is significant for the layers near the surface where the optical spectra originate, while at large depths ($\tau_{Ross} \geq 1$), the departure from LTE is small and so the LTE and NLTE atmospheric structures are similar.

One of the TLUSTY's output is the run of radiative acceleration with depth. As pointed out by Underhill (1949), there is minimum gravity at which the radiative pressure gradient becomes larger than $g/(k + \sigma)$; where g is the surface gravity, k is the mean absorption coefficient and σ is the scattering coefficient; so that the net gas-pressure gradient is negative; at such points the model may be dynamically unstable and large-scale mass motions may occur. In many ways this instability simply amounts to radial convection, but because the physical mechanism is so different from what is usually meant when one speaks of convection, it was referred to this as an instability against radiation pressure (or radiative acceleration).

Figures 3 and 4 show radiative acceleration computed for two gravities $\log g = 7$ and $\log g = 8$ and He/H = 10^3 for $T_{eff} = 60000$ K, $T_{eff} = 80000$ K,

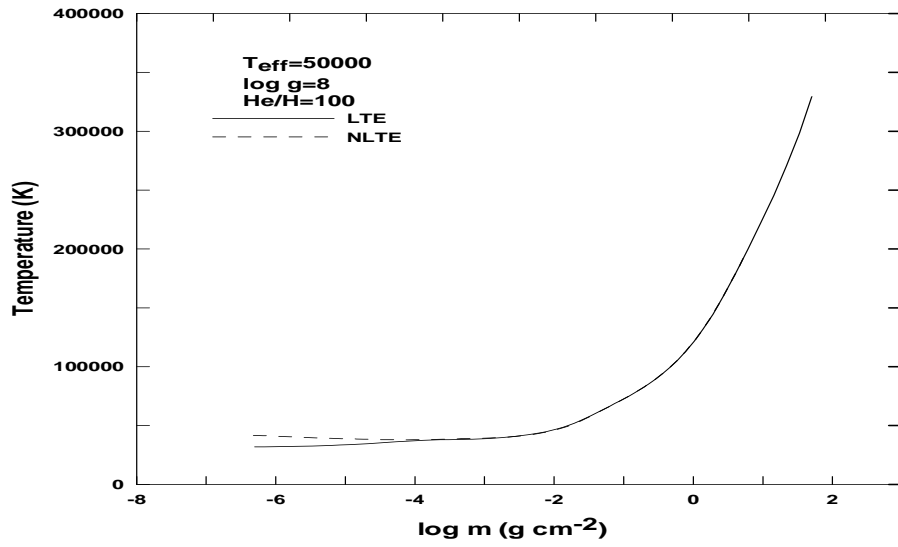


Figure 1. The temperature stratification for the NLTE model at 50000 K, $\log g = 8$, $\text{He}/\text{H} = 10^2$.

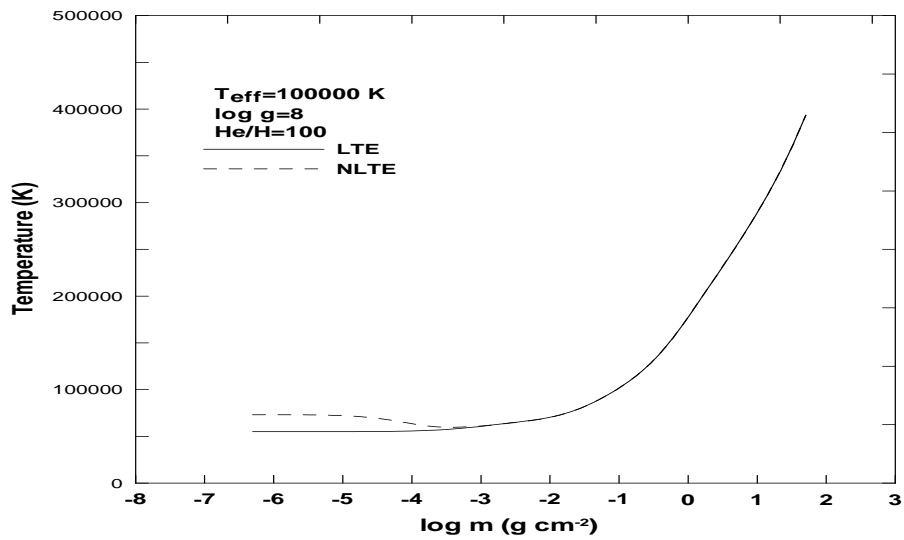


Figure 2. The temperature stratification for the NLTE model at 100000 K, $\log g = 8$, $\text{He}/\text{H} = 10^2$.

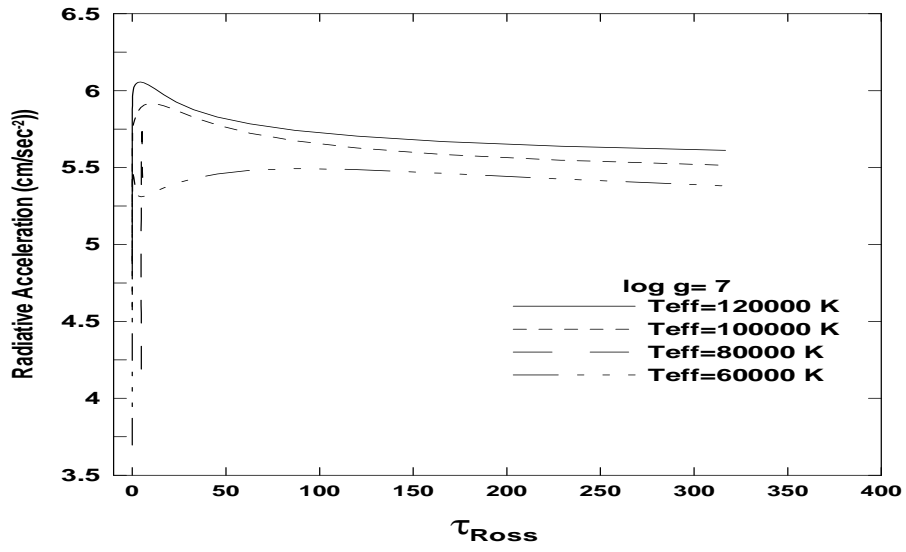


Figure 3. Radiative acceleration for NLTE models at $\log g = 7$.

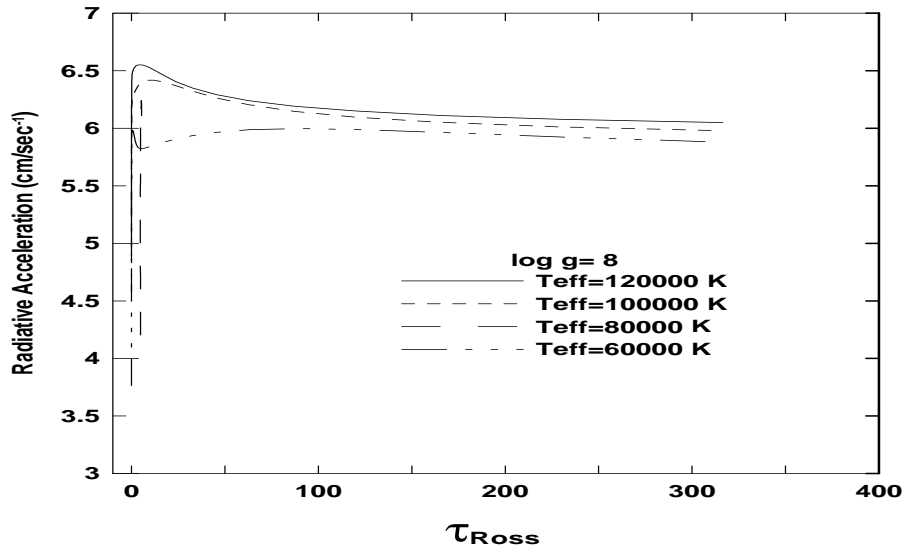


Figure 4. Radiative acceleration for NLTE models at $\log g = 8$.

$T_{eff} = 100000$ K and $T_{eff} = 120000$ K. As it is well shown, the radiative acceleration goes through a maximum in the continuum forming region ($\tau_{Ross} \approx 1$), with values smaller than the surface gravity, and then slowly decreases. This indicates that, although the lower atmospheric layers are more stable than the upper atmospheric layers, the assumption of the hydrostatic equilibrium is still valid.

3.2. Synthetic spectra

In this section we shall examine detailed synthetic spectra and line profiles calculated with SYNSPEC. Figure 5 shows the variations in the spectra with T_{eff} for the helium abundance $He/H = 10^3$. The flux is normalized to the continuum and shifted by an arbitrary value for more clarity. As shown, as we go high in the effective temperature, the HeI lines are weaker and at the same time the HeII lines become stronger. At $T_{eff} = 40000$ K, the HeII lines have nearly vanished, the He II 4686 Å line should start appearing at about 40 kK, and this spectrum would be classified as DB white dwarfs. The strength of He I 5870 Å varies detectably with the effective temperatures, so it could be used for the determination of them. Also, the nearly constant strength of He II 4686 Å line reflects the difficulties of determining the effective temperatures of DO white dwarfs. This behavior is obtained also by other authors, e.g. Wesemael et al. (1985).

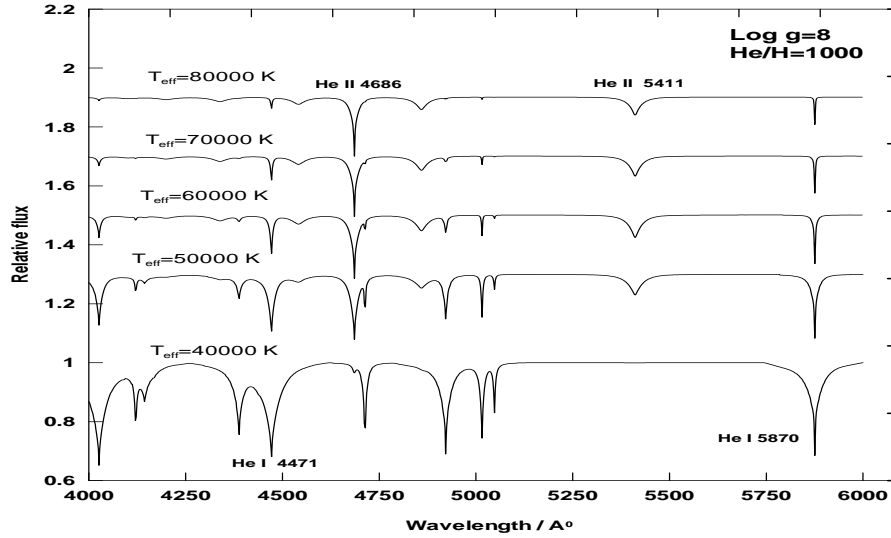


Figure 5. Dependence of representative spectra (computed from NLTE models) on T_{eff} .

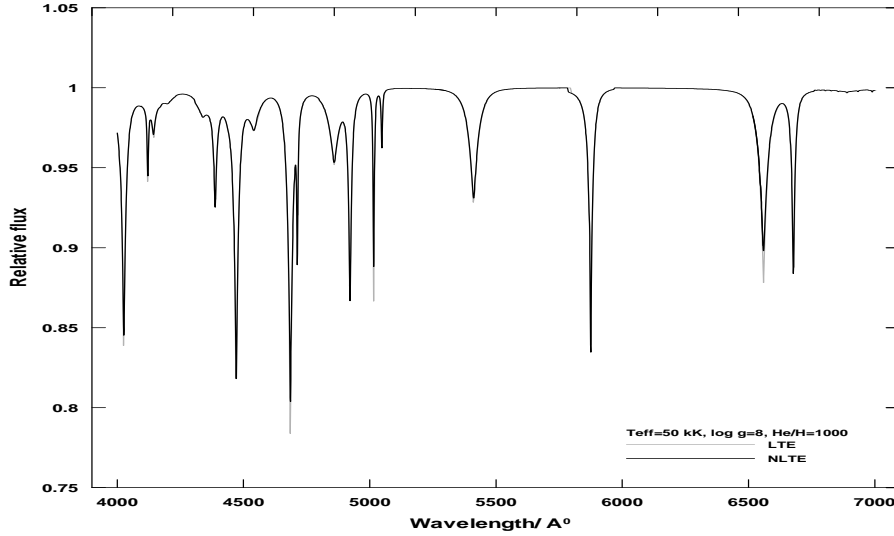


Figure 6. The effect of NLTE on the line profiles for model at $T_{eff}=50$ kK. Grey line stands for LTE and the black line for NLTE spectra.

As demonstrated by many authors (Napiwotzki, 1997 and Werner, 1996), NLTE models are required to analyze the spectra for DO white dwarfs. In Figures 6 to 9, we plotted synthetic LTE and NLTE line profiles for DO white dwarfs. The models are calculated at $T_{eff}=50$ kK, 60 kK, 70 kK and 80 kK. All models are calculated at $\log g=8$ and $\text{He}/\text{H}=10^2$. As it follows from the figures, the deviations between LTE and NLTE line profiles are strongly found for models at $T_{eff}=60$ kK and 70 kK, and there are little deviation for models at $T_{eff}=50$ kK and 80 kK.

Figure 10 shows the effect of gravity on the spectra for a star with $T_{eff} = 50000$ K and helium abundance $\text{He}/\text{H} = 10^3$. As it is clear the width of the He I 5870 Å line decrease with decreasing gravity, so, these lines are a good indicator for determination of gravity for cool DO white dwarfs.

To investigate the effect of increasing helium abundance on the line profiles we plotted the profiles of the two lines He I 4338 Å and He I 4860 Å in Figures 11, 12, 13 and 14. The line profiles are calculated at $T_{eff}=50$ kK and 80 kK, the two models are at $\log g=8$. We notice from the figures that for $T_{eff}=50$ kK there are smaller differences between the profiles calculated at $\text{He}/\text{H}=10^4$ and these calculated at 10^2 and 10^3 , but the profiles calculated at $\text{He}/\text{H}=10^2$ and 10^3 display the same shape. At $T_{eff} = 80$ kK, the profiles have almost the same shape for the three helium abundances. So, it is not an easy task to determine the hydrogen abundance in DO white dwarfs (Werner, 1996).

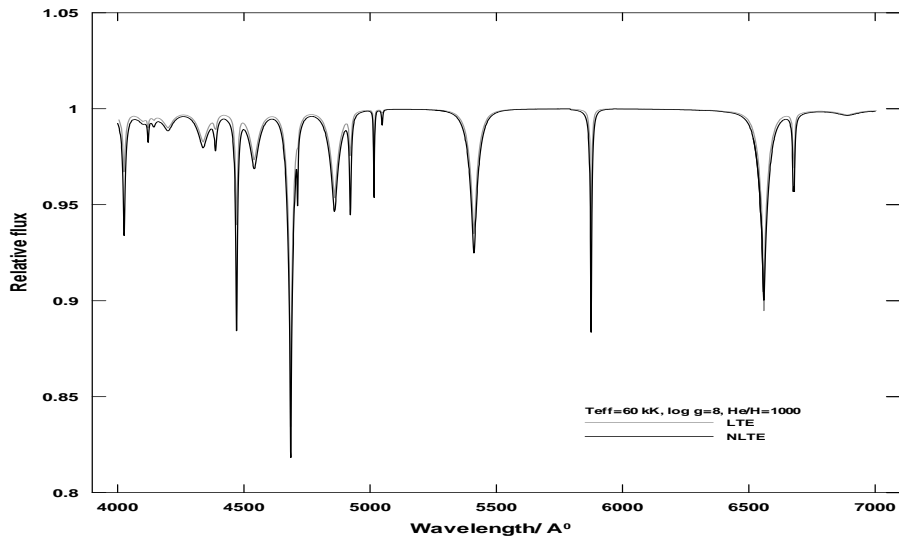


Figure 7. The effect of NLTE on the line profiles for model at $T_{eff}=60 \text{ kK}$. Grey line stands for LTE and the black line for NLTE spectra.

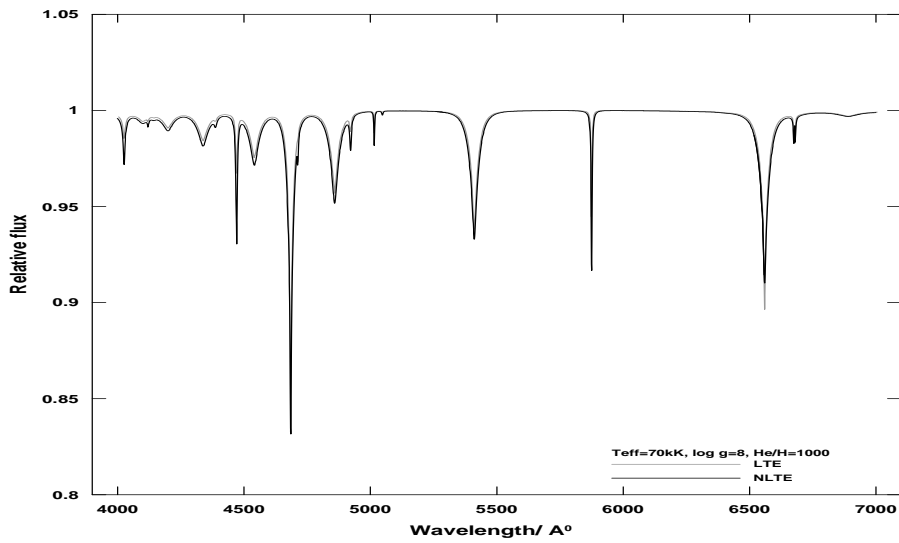


Figure 8. The effect of NLTE on the line profiles for model at $T_{eff}=70 \text{ kK}$. Grey line stands for LTE and the black line for NLTE spectra.

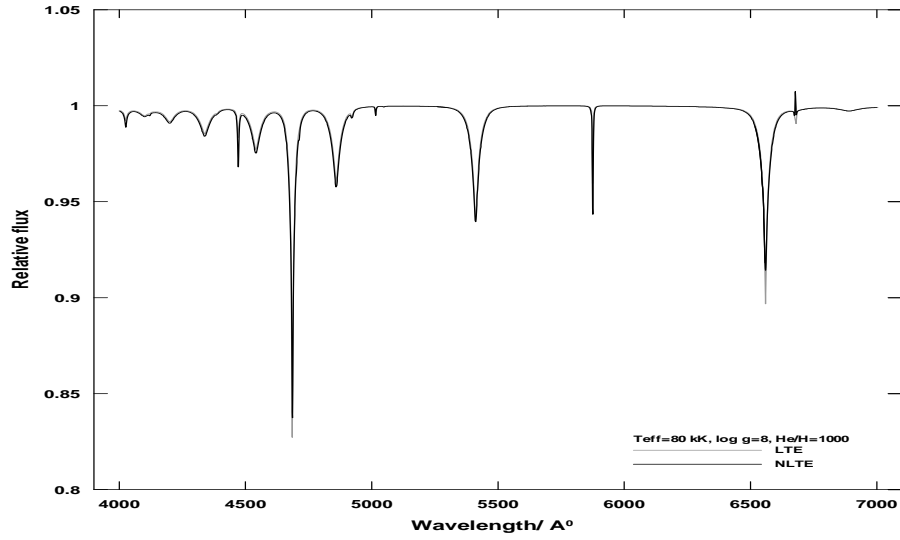


Figure 9. The effect of NLTE on the line profiles for model at $T_{eff}=80$ kK. Grey line stands for LTE and the black line for NLTE spectra.

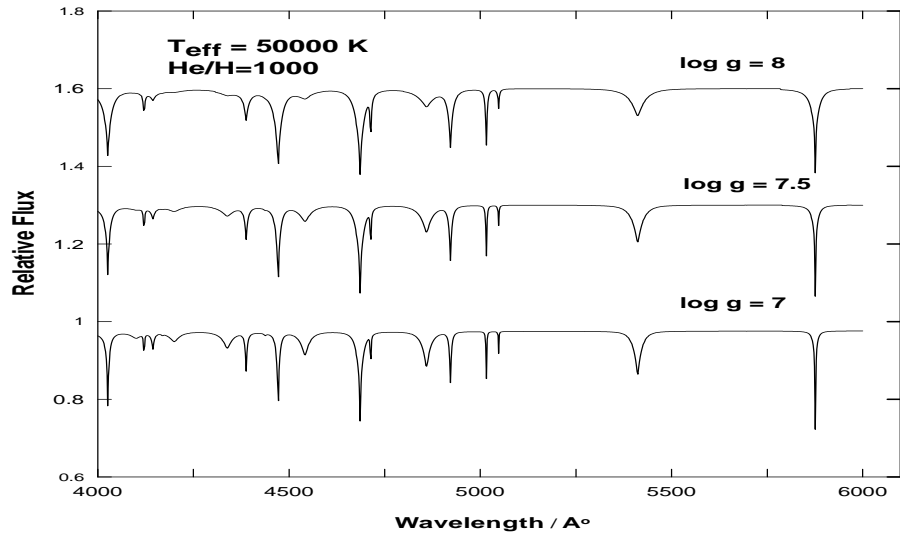


Figure 10. Dependence of representative spectra (computed from NLTE models) on gravity.

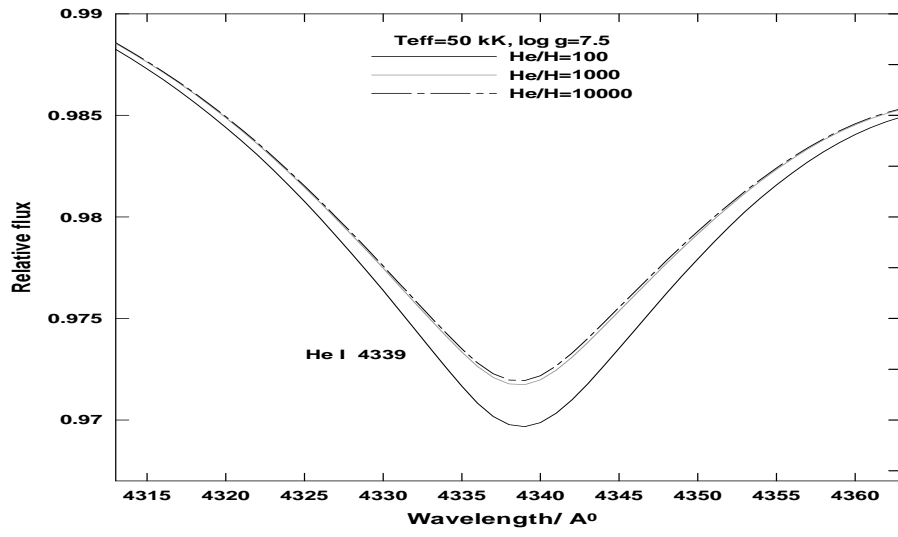


Figure 11. He I 4339 Å line profiles at different abundance, $T_{eff}=50$ kK and $\log g=7.5$.

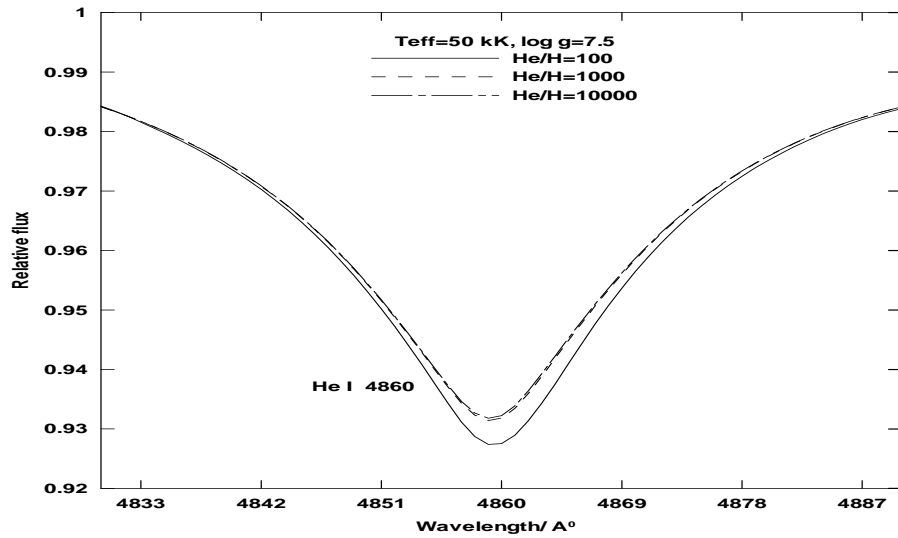


Figure 12. He I 4860 Å line profiles at different abundance, $T_{eff}=50$ kK and $\log g=7.5$.

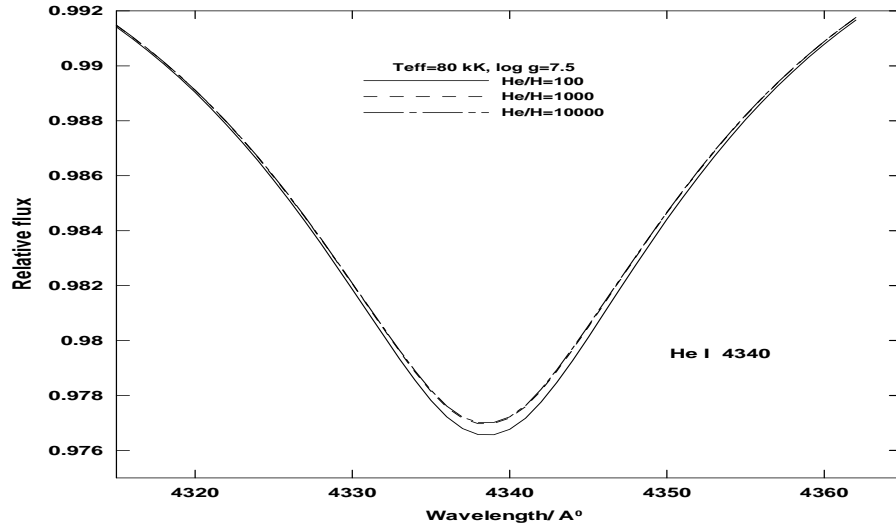


Figure 13. He I 4339 Å line profiles at different abundance, $T_{\text{eff}}=80 \text{ kK}$ and $\log g=7.5$.

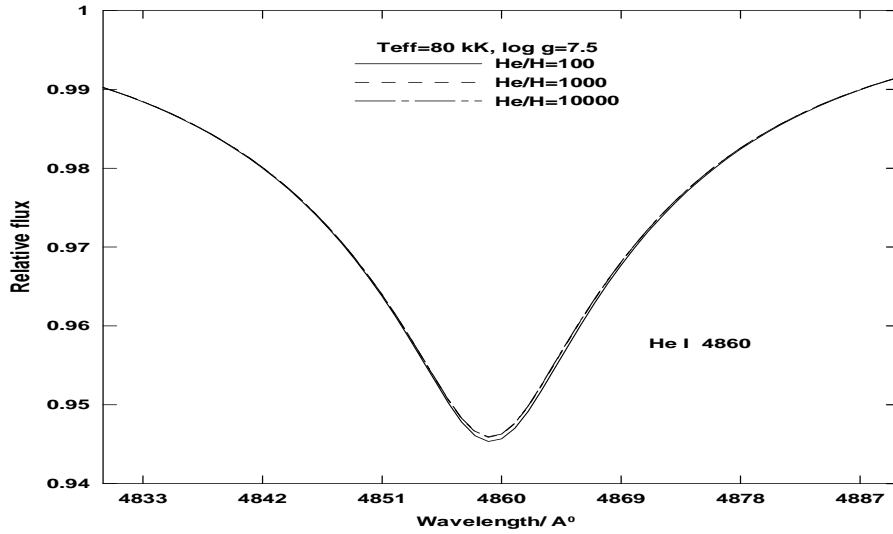


Figure 14. He I 4860 Å line profiles at different abundance, $T_{\text{eff}}=80 \text{ kK}$ and $\log g=7.5$.

4. Application to the observed spectra

4.1. Determination of the fundamental parameters

To determine the fundamental parameters of the observed spectra, by determining the best fit between the observed and the grid, three algorithms should be developed, the first is to adjust the spectral resolution and the second to bring the two spectra to a common wavelength scale and the third is devoted to the method of fitting.

Since the spectral resolution of the observed spectra is not the same as the grid, the synthetic spectra are brought to the same resolution by convolution.

The second step required to begin the comparison between the observed and grid spectra is adjusting of the wavelength scale. Since the radial velocity of the observed star is unknown, no valuable comparison can be made until the two spectra are properly shifted to be brought into the same reference system. We used cross-correlation method to determine lineshifts and radial velocities as

$$r = \frac{\frac{1}{n} \sum (F_i - \bar{F})(\phi_i - \bar{\phi})}{\sqrt{(\frac{1}{n} \sum (F_i - \bar{F})^2)(\frac{1}{n} \sum (\phi_i - \bar{\phi})^2)}}, \quad (1)$$

where ϕ_i are the observed spectra and F_i are the model spectra, and

$$\bar{F} = \frac{1}{n} \sum F_i, \quad \bar{\phi} = \frac{1}{n} \sum \phi_i.$$

This step was performed by transforming the wavelengths λ_i of both spectra into $\log \lambda_i$ and finding the $\sigma \log \lambda$ shift giving the highest correlation between the observed spectra and the spectra of the grid.

For the purpose of comparing the grid with the observed spectra, we have elaborated a code which minimizes the Euclidian distance between observed ϕ_i and template F_i fluxes as (Allende Prieto, 2004)

$$d = \sum w_i \mu_i, \quad (2)$$

where

$$\mu_i = [\phi_i - F_i(x)]^2,$$

and x is the vector of the fundamental parameters, i.e, T_{eff} , $\log g$ and He/H.

The weight w_i could be given by

$$w_i = \sum_i \frac{1}{I(x_i)} \left| \frac{\partial \mu_i}{\partial x_i} \right|, \quad (3)$$

where

$$I(x_i) = \sum_i \left| \frac{\partial \mu_i}{\partial x_i} \right|. \quad (4)$$

In the present calculations, we take $w_i = 1$, so we didn't need the interpolation between the flux grid.

4.2. Observations

We have used, as an application of the present grid, the DO observation from the Data Release Four (DR4) of SDSS. The SDSS is a photometric and spectroscopic survey covering 700 square degrees of the sky around the northern Galactic cap (Adelman-McCarthy et al., 2005). The main goal of the survey is to study the large scale structure of the universe. A small fraction of the observed stars are targeted for spectroscopy. The resulting data are in low resolution ($R = 1800$, $\text{FWHM} \simeq 3 \text{ \AA}$). The flux calibrated spectra cover the range between 3800 and 9000 \AA .

4.3. Application

Having built up the NLTE grid of synthetic spectra and the fitting algorithm we investigate the spectroscopic diagnostic tools developed from the grid.

Instead of line profile fitting, we have chosen a global fit to the optical spectrum of each star. Due to the blend of the most of the HeI lines with hydrogen lines and a nearly constant strength of HeII lines in the spectra of the DO white dwarfs, equivalent width and line profiles become not easy and less accurate task, so, we determined the fundamental parameters based on the shape and strength of all spectral features.

We have fitted the observed spectra with fixed He/H (10^4), that is because there is a very little effect of using variable He/H.

The resulting stellar parameters for the selected DO white dwarfs are presented in Table 1. The first row represents our result, whereas the second row presents the results of Hügelmeyer et al. (2005). The errors in the parameters are calculated employing an $1 - \sigma$ error algorithm by Zhang et al. (1986). Comparison between our result and Hügelmeyer et al. reveals a good agreement for the cooler stars while there is a small difference (within the errors in the parameters) for the hotter one. The best fitted model as well as the observed spectra are displayed in Figures 15 to 23.

5. Discussion and conclusion

We presented a grid of model atmospheres and synthetic spectra for hot helium-rich white dwarfs in order to elucidate the nature and characteristics of the progenitors of the DO white dwarfs. The grid coverage is $50000 \leq T_{eff} \leq 120000 \text{ K}$ with a step of 2500 K and $7 \leq \log g \leq 8.5$ with a step of 0.25 dex, for three helium abundance values (He/H): 10^2 , 10^3 and 10^4 . The spectra are synthesized with a sampling of 0.1 \AA and covering the wavelength range from 3000 to 7000 \AA .

Application of the present grid to the DO observation from the Data Release Four (DR4) is presented and reveals a good agreement for the cooler stars while there is a small difference for the hotter ones.

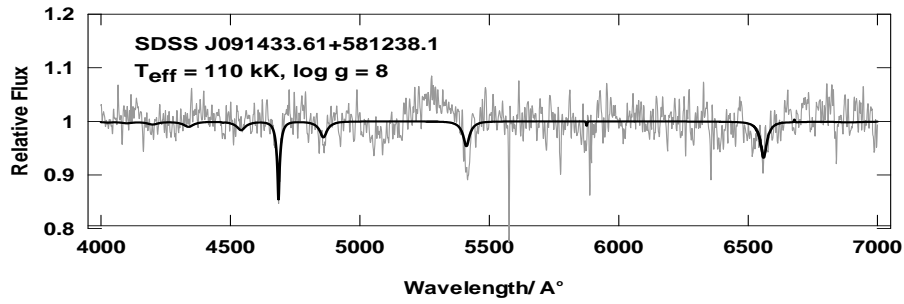


Figure 15. Normalized spectra of SDSS J091433.61+581238.1 (grey lines) along with model atmosphere fits (black lines).

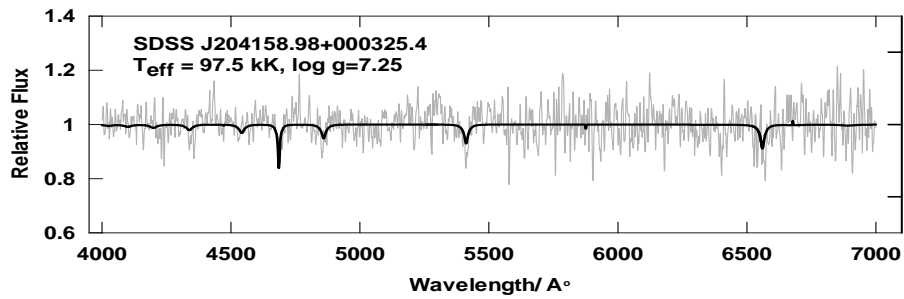


Figure 16. Normalized spectra of SDSS J204158.98+000325.4 (grey lines) along with model atmosphere fits (black lines).

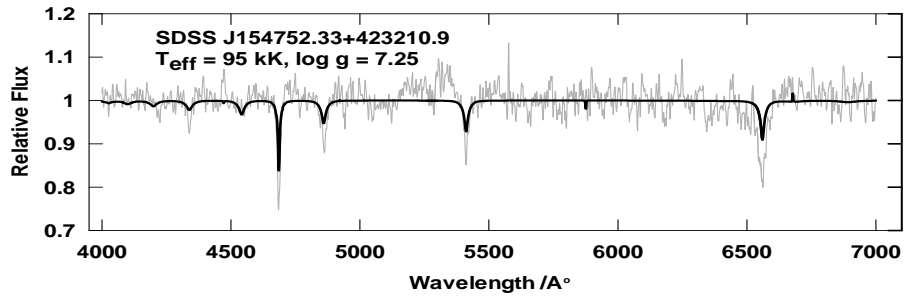


Figure 17. Normalized spectra of SDSS J154752.33+423210.9 (grey lines) along with model atmosphere fits (black lines).

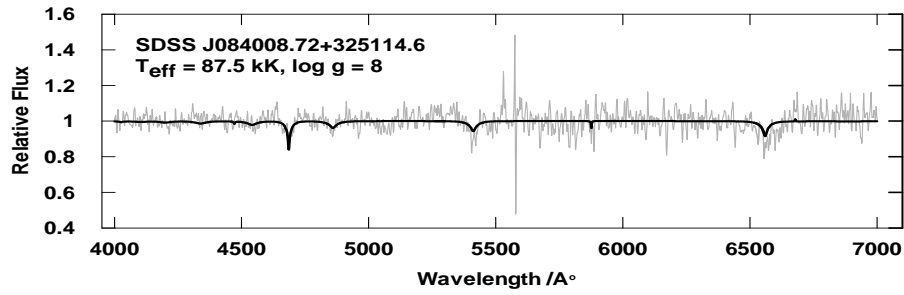


Figure 18. Normalized spectra of SDSS J084008.72+325114.6 (grey lines) along with model atmosphere fits (black lines).

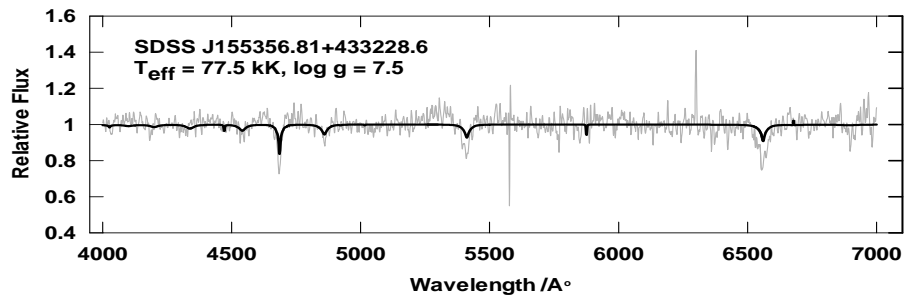


Figure 19. Normalized spectra of SDSS J155356.81+433228.6 (grey lines) along with model atmosphere fits (black lines).

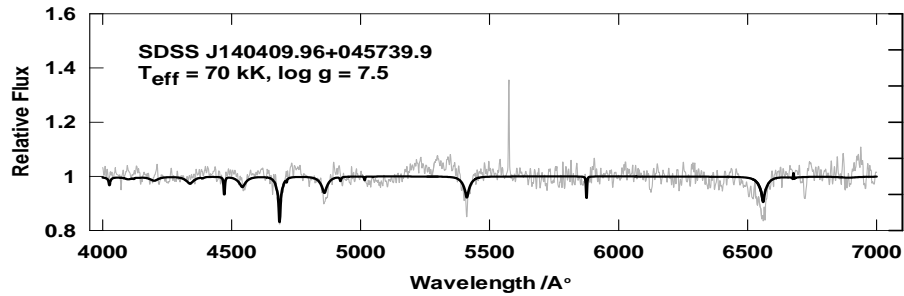


Figure 20. Normalized spectra of SDSS J140409.96+045739.9 (grey lines) along with model atmosphere fits (black lines).

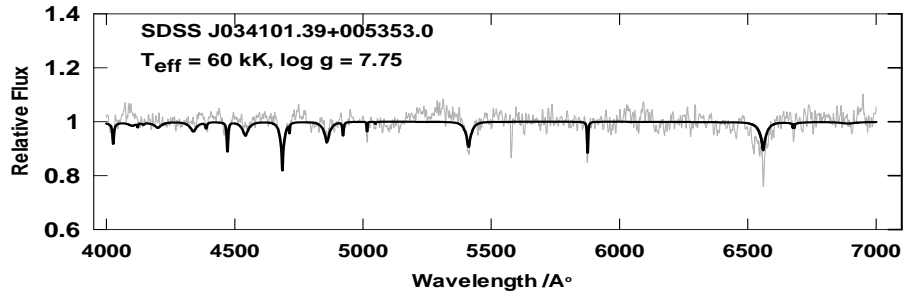


Figure 21. Normalized spectra of SDSS J034101.39+005353.0 (grey lines) along with model atmosphere fits (black lines).

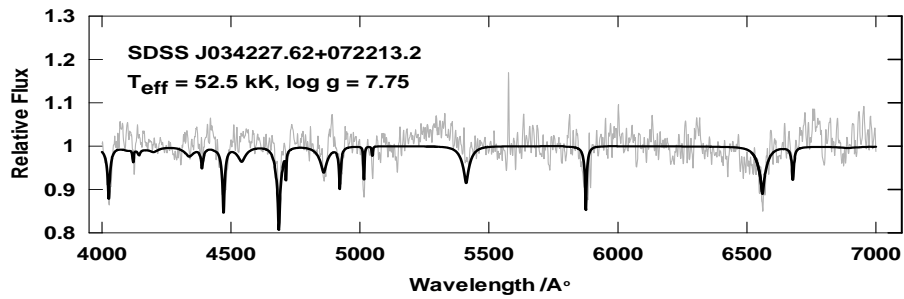


Figure 22. Normalized spectra of SDSS J034227.62+072213.2 (grey lines) along with model atmosphere fits (black lines).

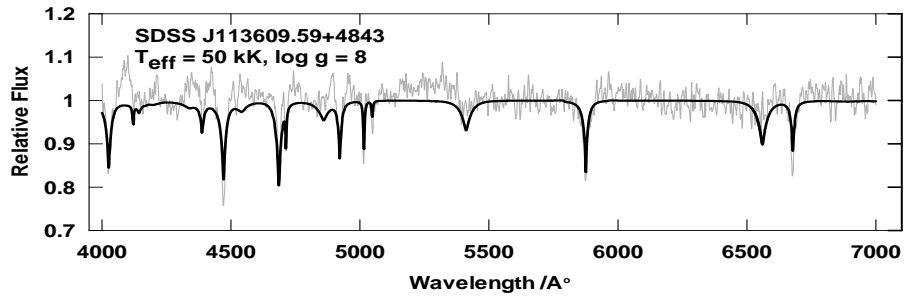


Figure 23. Normalized spectra of SDSS J113609.59+484318.9 (grey lines) along with model atmosphere fits (black lines).

Table 1. Fundamental parameters of the selected DO white dwarfs, for each star the first row represents our results, whereas the second row represents the results of Hügelmeyer et al. (2005) .

Name	T_{eff} [kK]	$\log g$ [cgs]
SDSS J091433.61+581238.1	110 ± 3.4	8 ± 0.17
	120 ± 4.1	8 ± 0.11
SDSS J204158.98+000325.4	97.5 ± 1.6	7.25 ± 0.081
	110 ± 4.4	7.2 ± 0.56
SDSS J154752.33+423210.9	95 ± 2.9	7.25 ± 0.14
	100 ± 3.7	7.6 ± 0.19
SDSS J084008.72+325114.6	87.5 ± 1.7	8 ± 0.084
	85 ± 3.7	8.4 ± 0.27
SDSS J155356.81+433228.6	77.5 ± 1.8	7.5 ± 0.092
	75 ± 4.0	8 ± 0.28
SDSS J140409.96+045739.9	70 ± 3.13	7.5 ± 0.15
	70 ± 1.7	8 ± 0.14
SDSS J034101.39+005353.0	60 ± 3.34	7.75 ± 0.16
	55 ± 8.4	8 ± 0.9
SDSS J034227.62+072213.2	52.5 ± 2.97	7.75 ± 0.14
	50 ± 0.5	8 ± 0.05
SDSS J113609.59+484318.9	50 ± 2.87	8 ± 0.14
	48 ± 0.3	8 ± 0.1

The fitted models to the observed spectra have many features. As we have mentioned above, the line profiles of DO white dwarfs are very difficult to fit. While the He I 5870 Å line represents a good indicator for the determination of both gravity and effective temperature, it is lost completely for $T_{eff} > 100000$ K. This behavior is also found by Werner (1994, 1996).

The above theoretical result is confirmed by the high S/N ratio observation of the DO white dwarfs PG1034+001 which reveals that due to the absence of the He I 5870 Å line, the temperature of the model fitted to the observation must be greater than 80000 K. As a result, the profiles of the other He lines become a poor fit.

Another problem encountered during the fitting process is the strength and shape of the He II 4686 Å line. In cool DO, the line is blended with the H_α line, while in the hot DO, the line have a constant strength.

According to these two problems, besides other difficulties when dealing with other lines, the importance of the continuous improvement of the broadening theories of the He II lines and a different grid of helium-rich models have been arisen.

Acknowledgments

Thanks go to the anonymous referee for his/her valuable comments which improved the scientific contents.

References

- Adelman-McCarthy, J. K., Agüeros, M. A., et al.: 2005, *ApJS* **162**, 38
 Allende Prieto, C.: 2004, *Astron. Nachr.* **325**, 604
 Dreizler, S., Werner, K.: 1996, *Astron. Astrophys.* **314**, 217
 Hubeny, I., Hummer, D., Lanz, T.: 1994, *Astron. Astrophys.* **252**, 151
 Hubeny, I.: 1988, *Comp. Phys. Commun.* **52**, 103
 Hubeny, I., Lanz, T.: 1992, *Astron. Astrophys.* **262**, 501
 Hubeny, I., Lanz, T.: 1995, *Astrophys. J.* **439**, 875
 Hubeny, I., Lanz, T.: 2003, in *Stellar Atmospheres Modeling*, eds.: I. Hubeny, D. Michalás and K. Werner, ASP Conf. Ser. 288, San Francisco, 51
 Hügelmeyer, S., Dreizler, S., Werner, K., Krezesinski, J., Nitta, A., Kleinman, S.: 2005, *Astron. Astrophys.* **442**, 309
 Koester, D.: 2002, *Ann. Rev. Astron. Astrophys.* **11**, 33
 Kubat, J.: 1995, *Astron. Astrophys.* **299**, 803
 Kubat, J.: 1997, *Astron. Astrophys.* **324**, 1020
 Lanz, T., Hubeny, I., Heap, S. R.: 2003, in *Modelling of Stellar Atmospheres*, eds.: N.E. Piskunov, W. W. Weiss and D.F. Gray, IAU Symposium 210, San Francisco: ASP, 67
 Lanz, T., Hubeny, I.: 2006, <http://arxiv.org/pdf/astro-ph/0611891v1>
 Napiwotzki, R.: 1997, *Astron. Astrophys.* **322**, 256
 Underhil, A.: 1949, *Mon. Not. R. Astron. Soc.* **109**, 562
 Werner, K.: 1996, *Astron. Astrophys.* **309**, 861
 Werner, K., Heber, U., Fleming, T.: 1994, *Astron. Astrophys.* **284**, 907
 Werner, K., Dreizler, S., Wolf, B.: 1995, *Astron. Astrophys.* **298**, 567
 Wesemael, F.: 1981, *Astrophys. J., Suppl. Ser.* **45**, 177
 Wesemael, F., Green, R., Liebert, J.: 1985, *Astrophys. J., Suppl. Ser.* **58**, 379
 Zhang, E.-H., Robinson, E., Nather, R.: 1986, *Astrophys. J.* **305**, 740